Toehold-mediated strand displacement to measure released product from self-cleaving ribozymes

JAY BHAKTI KAPADIA,[1,2] NAWWAF KHARMA,[1,3] ALEN NELLIKULAM DAVIS,[1] NICOLAS KAMEL,[1] and JONATHAN PERREAULT[2,3]

[1]Electrical and Computer Engineering Department, Concordia University, Montreal, Quebec, Canada H3G 1M8
[2]INRS-Centre Armand-Frappier Santé Biotechnologie, Laval, Quebec, Canada H7V 1B7
[3]Centre for Applied Synthetic Biology (CASB), Concordia University, Montreal, Quebec, Canada H4B 1R6

ABSTRACT

This paper presents a probe comprising a fluorophore and a quencher, enabling measurement of released product from self-cleaving hammerhead ribozyme, without labeled RNA molecules, regular sampling or use of polyacrylamide gels. The probe is made of two DNA strands; one strand is labeled with a fluorophore at its 5′-end, while the other strand is labeled with a quencher at its 3′-end. These two DNA strands are perfectly complementary, but with a 3′-overhang of the fluorophore strand. These unpaired nucleotides act as a toehold, which is utilized by a detached cleaved fragment (coming from a self-cleaving hammerhead ribozyme) as the starting point for a strand displacement reaction. This reaction causes the separation of the fluorophore strand from the quencher strand, culminating in fluorescence, detectable in a plate reader. Notably, the emitted fluorescence is *proportional* to the amount of detached cleaved-off RNAs, displacing the DNA quencher strand. This method can replace or complement radio-hazardous unstable ^{32}P as a method of measurement of the product release from ribozyme cleavage reactions; it also eliminates the need for polyacrylamide gels, for the same purpose. Critically, this method allows to distinguish between the total amount of cleaved ribozymes and the amount of *detached* fragments, resulting from that cleavage reaction.

Keywords: inducible ribozyme; allosteric ribozyme; product dissociation; synthetic biology

INTRODUCTION

Nucleic acid strand displacement reactions make DNA and RNA into powerful tools for the design of various molecular motors (Yurke et al. 2000), biosensors and amplifiers, as well as a means of molecular computation akin to digital circuits and neural networks (Qian and Winfree 2011; Qian et al. 2011; Wang et al. 2018). DNA is often the material of choice for building nano circuits, amplifiers and molecular probes, often preferred over RNA due to DNA's robustness and ease of production and manipulation (Zhang and Winfree 2009). Toehold-mediated strand displacement reactions (TMSDRs) are widely used to determine single nucleotide polymorphisms and in constructing DNA-based logic circuits (Khodakov et al. 2015; Ravan et al. 2020). The specificity of TMSDRs lie in nucleic acid sequence dependency. TMSDRs are often more sensitive to base-pair mismatches than some of the other classical hybridization reactions (Duose et al. 2012), making it appropriate for detection of specific RNA and DNA sequences.

Hammerhead ribozymes (HHRs) are nonproteinaceous RNA motifs that can catalyze transesterification reactions (Prody et al. 1986; Hammann et al. 2012; Scott et al. 2013). HHRs can be found in plant RNA viruses, satellite RNA, viroids and repetitive satellite DNA (Hammann et al. 2012). HHRs require a minimum of ~50 nt to form a two-dimensional structure resembling a hammerhead and that can catalyze strand scission reactions (Murray et al. 1998; Chi et al. 2008; Nelson and Uhlenbeck 2008). Synthetic HHRs are capable of cleaving RNA strands in *trans*; however, known HHRs also demonstrate *cis* activity (Scott et al. 2013). In nature, there exists (at least) three types of HHRs, depending on the positions of loops (Hammann et al. 2012). For example, type I HHR has loops in both stems II and III, but not in stem I, as shown in Figure

Corresponding authors: kharma@ece.concordia.ca, jonathan.perreault@inrs.ca
Article is online at http://www.rnajournal.org/cgi/doi/10.1261/rna.078823.121.

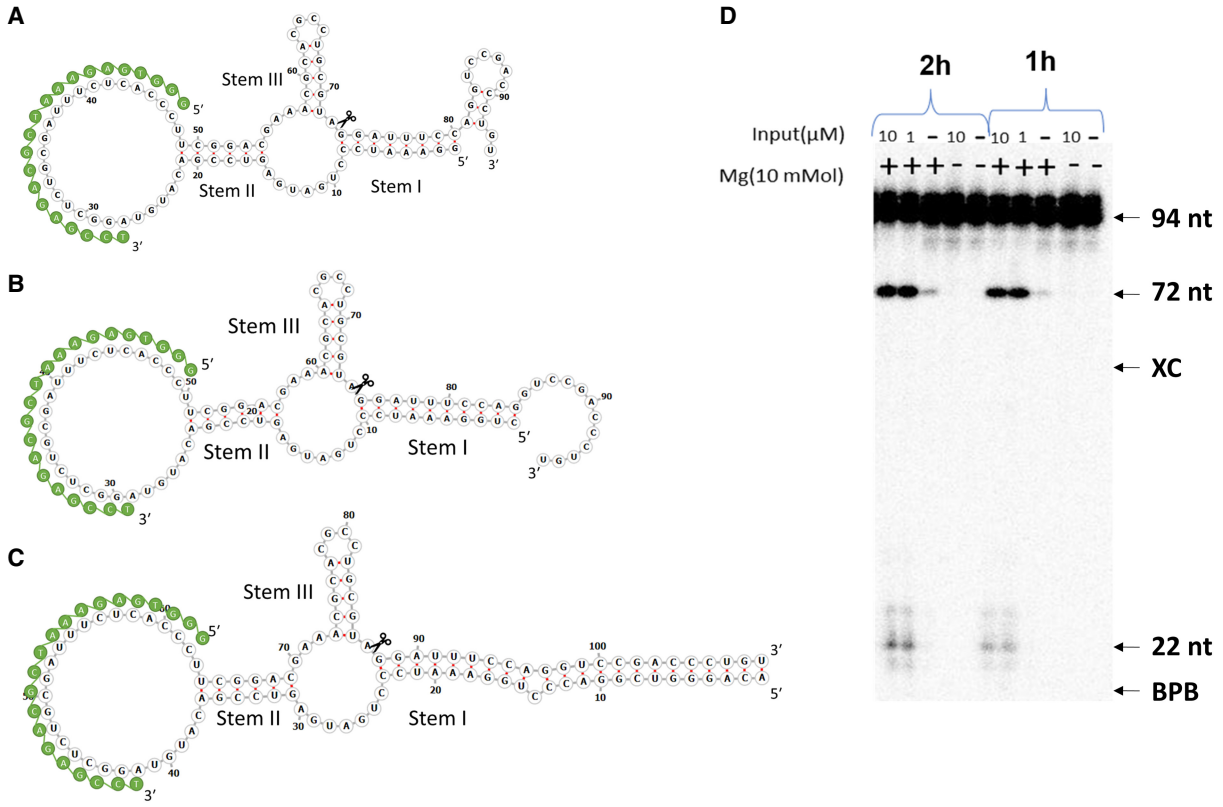

FIGURE 1. Different active HHR secondary structures, with different amounts of base-pairing in stem I between the still-attached output strand and its complement. The green strand represents the input DNA oligonucleotide for all ribozymes (5′-GGGTGAGAAATCGCAGAGCCTA-3′). (*A*) Schematic diagram of a YES logic gate with 8 bp in stem I. (*B*) A YES logic gate with 10 nt of base-pairing in stem I (8 + 2 bp). (*C*) a YES logic gate with 22 nt of base-pairing in stem I (8 + 14 bp). (*D*) Ribozyme illustrated in *A* cleavage in different conditions: Lanes from *left* to *right*: (First lane) Ribozyme without Mg^{2+} and input DNA. (Second lane) Ribozyme + 10 μM DNA without Mg^{2+}. (Third lane) Ribozyme + Mg^{2+} 10 mM. (Fourth lane) Ribozyme + Mg^{2+} + 1 μM input DNA. (Fifth lane) Ribozyme + Mg^{2+} + 10 μM input DNA. Reaction was stopped at 1 and 2 h with denaturing buffer (containing 80% formamide, 0.5 M EDTA, 0.002% bromophenol blue and 0.002% xylene cyanole). All ribozyme secondary structures were generated using Forna-RNA web server (Kerpedjiev et al. 2015). Even if the 20 bp complementarity between input DNA and loop II of HHR is likely to impede stem II formation and thus activity, compared to so-called natural extended HHRs, it is nevertheless required for activity by design.

1A–C. HHRs can be designed to be induced by single-stranded RNA (ssRNA) molecules, single-stranded DNA (ssDNA) molecules or, in the case of aptazymes, by small molecules such as tetracycline (Penchovsky and Breaker 2005; Wittmann and Suess 2011). Using these HHRs, different types of logic gates can be (and have been) designed, activated by one or more inputs including ssDNA and ssRNA (Penchovsky and Breaker 2005; Wittmann and Suess 2011). Most ribozyme cleavage assays are performed using polyacrylamide gels and radiolabeling, as described in Figure 1D.

As illustrated in Figure 2A and B, a YES logic gate can be described as a single input gate, which is activated upon introduction of input DNA in the medium. In this study, HHRs were designed to respond to specific nucleic acid sequences (inputs). Upon binding with such inputs, these HHRs refold into their active form. This active form catalyzes a strand-cleavage reaction, leading to the production of a small ssRNA fragment called "output." Our designed ribozyme indeed behaved as YES logic gate, as shown by the polyacrylamide gel (Fig. 1D).

Evaluating the kinetics of ribozyme cleavage reactions is essential to understanding their mechanisms of operation, for characterizing mutants and for estimating certain parameters critical to proper functioning of RNA-based circuits, such as cleavage rate. Generally, ribozyme kinetics are monitored using a radioisotope of ^{32}P that can be incorporated during transcription or posttranscriptionally using a polynucleotide kinase enzyme (Penchovsky and Breaker 2005; Wittmann and Suess 2011; Hammann et al. 2012). In addition to certain disadvantages, such as limited half-life and radiation hazard, the use of radioisotopes for this procedure limits it to laboratories with appropriate facilities. These facilities are becoming less common since fluorescence is increasingly replacing radioactivity as a preferred method of labeling. Other groups (e.g., Li et al. 2005) demonstrated HHR kinetics using fluorescence, where RNA molecules were labeled with cyanine-AMP

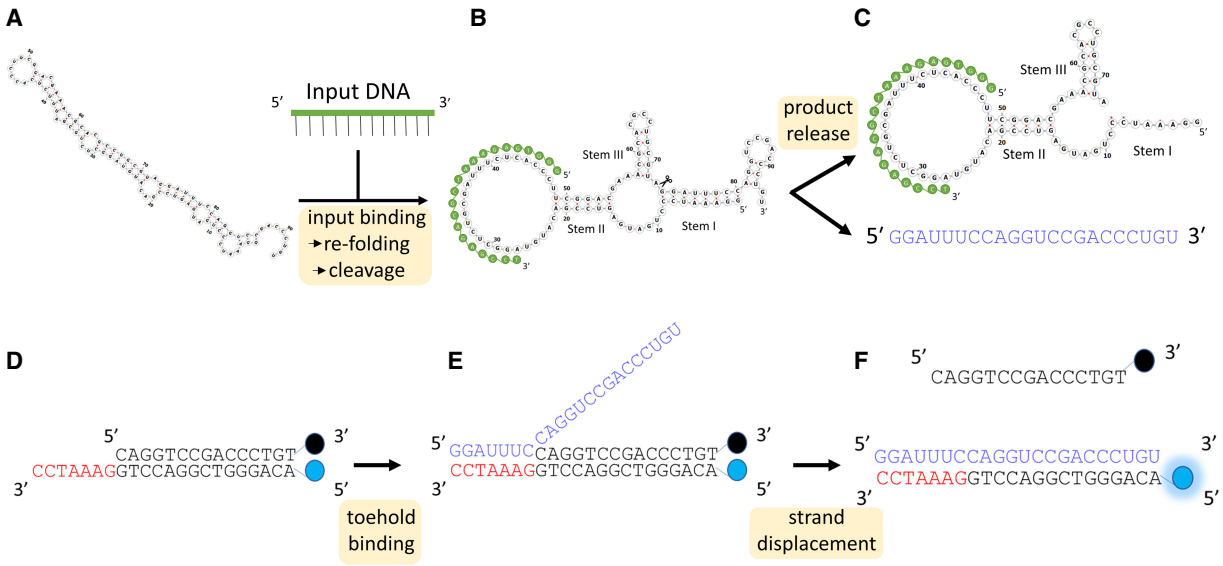

FIGURE 2. Schematic representation of the toehold-mediated strand displacement reaction used in measuring the kinetics of hammerhead ribozyme cleavage reactions. (*A*) Misfolded HHR in the absence of input. (*B*) The introduction of input DNA oligo (green strand) induces the formation of an active HHR core, resulting in cleavage activity (*C*) Cleavage products: cleaved HHR bound to input and released output (blue strand). (*D*,*E*) Released output interacting with toehold present on preannealed probe; this interaction results in the displacement of the Q-strand (orange strand). (*F*) Displacement of the Q-strand results in the separation of the quencher from the fluorophore, culminating in detectable fluorescence. All ribozyme figures were generated using Forna-RNA web server (Kerpedjiev et al. 2015).

during transcription. However, this process entails RNA modifications, causing fluctuations in the annealing temperature, which affect RNA folding and hence, ribozyme activity (Li et al. 2005; Scott et al. 2013; Moreira et al. 2015).

In this study, we describe a novel approach to detect released product from HHR cleavage using the toehold-mediated strand displacement reaction (TMSDR). A previously characterized YES logic gate is used to investigate the functionality of the novel TMSDR method (Fig. 1A). Upon binding to the input strand, the inactive ribozyme (Fig. 2A) folds into its active conformation (Fig. 2B), leading to HHR self-cleavage and to the release of a small 22 nt ssRNA "output strand" (Fig. 2C, bottom). When this output strand binds to the fluorescent strand of a specifically designed probe (Fig. 2D,E), the quencher strand is displaced, leaving the fluorophore free to fluoresce (Fig. 2F, bottom). The concentration of the cleaved-off RNA fragments dissociated from the ribozyme is determined using a standard curve.

RESULTS

Probe design and workflow of probe-mediated hammerhead kinetics

The ribozyme is designed to be *inactive* by default, then turn *active* when bound to an input strand. The secondary structure of the inactive form of the ribozyme is shown in Figure 2A. Once the input strand is bound to the oligonucleotide binding site (OBS) of the ribozyme, the ribozyme refolds into an active conformation (Fig. 2B) causing self-cleavage. Ribozyme self-cleavage releases the output strand (Fig. 2C), which binds progressively to the toehold of the probe (Fig. 2E,F). A few assays (data not shown) revealed that a toehold of 7 nt is sufficient to displace the quenching Q-strand. The probe is designed so strand displacement proceeds from the 5′-end to the 3′-end of the Q-strand, as this has been established to be the most efficient route to displacement (Šulc et al. 2014; Simmel et al. 2019). At the conclusion of the strand-displacement reaction, the quencher fully separates from the fluorophore, allowing the Cy5 to fluoresce.

Evaluation of HHR kinetics via a strand displacement reaction utilizing a fluorescent probe

The assessment of HHR kinetics using radiolabeling is very useful for determining the concentrations of cleaved ribozymes using denaturing PAGE, but the latter is less appropriate to determine the cleaved detached RNA outputs. This is because a gel shows all output strands of equal length in the same band, whether these strands have actually detached from the rest of the ribozyme or not, post cleavage. In addition, this method is time consuming and involves the use of radioisotopes, which are carcinogenic (Furth and Tullis 1956). To overcome these limitations, we sought to evaluate HHR kinetics using predesigned fluorescent probes.

As expected, fluorescence intensity increases with time in the assay group (HHR with input and Mg^{2+}) (Fig. 3A) and

little or no change in fluorescence intensity was noticed in either the background group or the HHR alone group (Fig. 3A). Conversely, for both HHRs with a longer stem I (+2 and +14 bp) assay groups, the observed fluorescence was near background levels. Taken together, these results provide evidence that the cleaved output from the original ribozyme binds to the toehold, displaces the Q-strand, leading to the observed fluorescence.

Furthermore, to determine the concentration of HHR output, we generated a standard curve using an R-strand equivalent to the output strand (Fig. 3B). Different concentrations of R-strands were mixed in with the probe and assayed using a fluorescent plate reader. The TMSDR fluorescence increased as a function of increased R-strand concentration. Thus, the generated standard curve can be utilized to interpolate the fluorescence values obtained from the TMSDR assay and hence, determine the concentration of detached output strand, generated by ribozyme self-cleavage.

Interpolated values were plotted for all three ribozymes (Fig. 3C). The original ribozyme (stem I of 8 bp, Fig. 1A) shows the highest activity level (as determined by TMSDR) relative to HHRs with a stem I of 10 bp or 22 bp (Fig. 3C). The original ribozyme has only 8 bp in stem I, joining the output strand to its complementary strand (Fig. 1A). The TMSDR results (Fig. 3A) show a decrease in fluorescence as a function of increased base-pairing with the output strand.

Kinetics of ribozyme cleavage with radiolabeled RNA

From previous studies, it has been shown that the radiolabeling of RNA molecules constitutes one of the best approaches to investigating RNA structure and function, in vitro (Celander and Cech 1991; Sclavi et al. 1998; Li et al. 2005). To investigate the cleavage of HHRs in the presence of inputs, HHRs are labeled with [α-^{32}P] UTP during transcription, incubated in a cleavage buffer, and the reaction is sampled (and stopped) at different time-points, to provide inputs to a polyacrylamide gel display. To provide further evidence in support of the claim, the original ribozyme (Fig. 2A) was modified at the 5′-end to increase base-pairing between the expected output strand and its complementary strand in stem I. Two of those ribozymes were designed (Fig. 1B,C), and then assayed alongside the original ribozyme, using the radiolabeling approach (Supplemental Fig. S2). The completed gel exhibits comprehensive data on the time of the cleavage reactions. In Supplemental Figure S2, the two major bands of each gel image correspond to the size of the full-length ribozyme and its cleaved product. For the original ribozyme (stem I of 8 bp) the two bands indicate 94 and 72 nt; for the HHR with an added 2 bp (10 bp) in stem I, they indicate 96 and 74 nt; for the HHR with an added 14 bp (22 bp) in stem I they indicate 108 and 86 nt. An increase in band intensity with time was measured for the cleavage products of all three ribozymes (also shown in Supplemental Fig. S2). The intensity of these bands was used as a measure of percentage of cleaved ribozyme: this is equal to the ratio of cleaved product (Cleaved ribozyme + Output fragment) over cleaved product plus full-length ribozyme (Uncleaved ribozyme + Cleaved ribozyme + Output fragment).

As expected, there was a gradual increase of fraction cleaved with time, for all three ribozymes (Fig. 4A). These results indicate that the input sequence does indeed induce HHR cleavage, under typical cleavage conditions (i.e., in the presence of Mg^{2+}). This shows that the designed HHRs have functioned as YES logic gates, in response to their intended input (Fig. 1D; Supplemental Fig. S2). Figure 1D shows the Mg^{2+} without DNA oligo control for the ribozyme. As an unintended result, we also found that the cleavage efficiencies of the different ribozymes were markedly different (Fig. 4A). We hypothesize that this was due to different interactions between the unpaired segment of stem I and the rest of the ribozyme; testing this hypothesis and characterizing the exact nature of such possible interactions fall outside the scope of this study.

Comparison of measurement of HHR cleavage reactions using conventional gels versus TMSDR

To better evaluate the output concentration derived from the conventional approach (gel) and the new probe approach (TMSDR), we compared cleavage activity measured by gel band intensity with cleavage activity as reflected by probe fluorescence (Fig. 4A). These results indicated that the two approaches measure the progress of cleavage reactions in different ways and provide complementary information: breakage of the phosphodiester linkage at the cleavage site measured with the denaturing gel vs. amount of dissociated products measured by TMSDR.

As demonstrated in Figure 4B, the cleavage from the gel is comparable with cleavage derived from the TMSDR assay in the case of the original ribozyme (normalized). However, as the base-pairing with the output strand increases, even by as little as 2 nt, the amount of released output decreases considerably, as illustrated by the green and blue bars representing the HHR with a stem I extended to 10 bp (I-10 bp) and 22 bp (I-22), respectively. The k_{obs} of the I-8, I-10 and I-22 HHRs were somewhat similar for gel-based assays (0.0046 min^{-1} [CI95: 0.0037 to 0.0054], 0.007 min^{-1} [0.002 to 0.012] and k_{obs} 0.012 min^{-1} [CI95: 0.004 to 0.022], respectively), but they appeared drastically different for TMSDR assays (0.0008 min^{-1} [CI95: 0.0006 to 0.0010], 0.00020 min^{-1} [CI95: 0.00005 to 0.00035] and 4.0×10^{-5} min^{-1} [CI95: 0.2×10^{-5} to 7.8×10^{-5}], respectively, for the I-8, I-10 and I-22 HHRs). It should be noted that the TMSDR-based k_{obs} calculation for the latter two (10 and 22 bp stem I) is prone to error due to the very weak cleavage. Still, the difference between gel-based and

TMSDR-based k_{obs} determination is within an order of magnitude for I-8, but shows a ~30-fold and ~3000-fold decrease, for I-10 and I-22, respectively; further supporting the comparison as shown in Figure 4B. It is important that the experimenters understand that and hence, utilizes the method most appropriate to the particular needs of their own projects.

Additional TMSDR assay with a Mn^{2+}-induced HHR

The previously published A6C mutation in the core of a HHR (Fig. 5A) was shown to have a k_{obs} of 0.18 min^{-1} in the presence of Mn^{2+} (Naghdi et al. 2020), much faster than the 0.005 min^{-1} of the example described above (Fig. 1A). Thus, this "Mn^{2+}-HHR" (Fig. 5A) was a good candidate to provide an additional example for TMSDR assay which is much faster and induced in a different way. A few bases were added at this ribozyme 3′ end to facilitate the output binding with the probe. The second fluorophore and quencher pair were used to demonstrate the versatility of the technique (BHQ-2 and Cy-3). As expected, the fluorescence increases with time when the Mn^{2+}-HHR is induced with $MnCl_2$ compared to the one without $MnCl_2$ (Fig. 5B). Standard curve for Mn^{2+} HHR probe was generated (Fig. 5C) according to the probe calibration in methods section. Converting to % of product release indicates that ~25% of the cleavage product is released (Fig. 5D) and that it appears to be the limiting step, as the previously reported k_{obs} of 0.18 min^{-1} is higher than the one calculated by TMSDR (k_{obs} of 0.068 min^{-1}), which is likely an overestimate considering that the cleavage reaction actually started ~2 min before the first fluorescence scans could be performed. Fluorescence values were normalized using the 10-min time point from the standard curve as reference. The fluorescence for this assay was normalized because of the photobleaching of Cy-3 (as seen from the + control for fluorescence, Fig. 5B), normalized and unnormalized fluorescence values are shown in Figure 5B, inset.

DISCUSSION

In the past three decades, several methods have been developed and used to analyze and evaluate the structure, functions and activity of ribozymes in vitro. These methods include RNA radiolabeling, posttranscriptional fluorescence labeling, phosphoramidite chemistry for fluorescent labeling and engineered fluorescent aptamers (e.g., Spinach and Mango) (Li et al. 2005; Porecha and Herschlag 2013; Auslander et al. 2016; Mitra and Ha 2019; Debiais et al. 2020). These techniques make use of transcriptional incorporation of [α-^{32}P] UTP, 5′-incorporation of ^{32}P from [γ-^{32}P] ATP or fluorophore, chemical synthesis of RNA and fluorescence activity of aptamers (Singh et al. 1999; Li et al. 2005; Porecha and Herschlag 2013; Auslander et al. 2016). Some of these labeling methods allowed very precise analysis

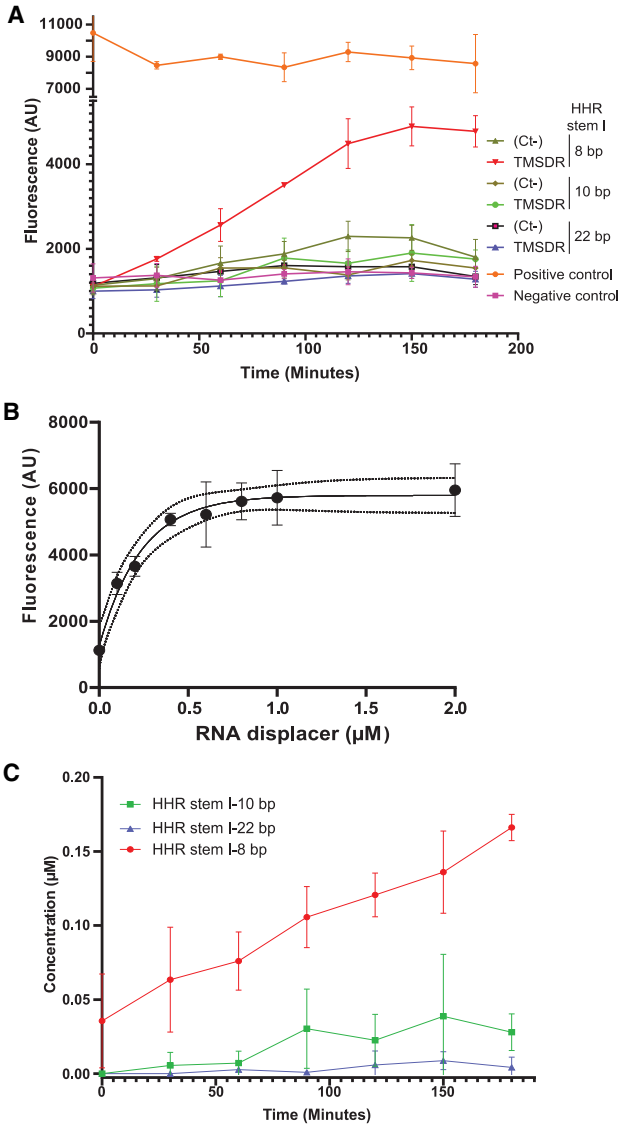

FIGURE 3. Analysis of the YES gate using probe (with Cy-5 as fluorophore and Black hole quencher-2 as quencher). (*A*) 0.5 μM of probe and 1 μM of ribozyme were used in the assay. A total of 10 μM of the R-strand with the probe was used as positive control (i.e., a probe unquenched by a large excess of R-strand), and a quenched probe was used as negative control. Ribozyme without Mg^{2+} and without input DNA was used as another negative control (Ct−). The assay group includes 10 μM input DNA and 10 mM Mg^{2+}. Readings were taken every 30 min over a period of 180 min. The same protocol was followed for HHR with a stem I of either 10 bp (I-10) or 22 bp (I-22). (*B*) The standard curve for the 0.5 μM probe uses the same reagents as for the assay. Different concentrations of the RNA displacer strand were used (0.05, 0.1, 0.2, 0.4, 0.6, 0.8, 1, and 2 μM). (*C*) Interpolated fluorescence values from the three ribozyme assays mapped using a standard curve to concentrations of released output strand, for the same three ribozymes. A similar experiment which includes the control "no input, with Mg^{2+}" is provided in the Supplemental Material (Supplemental Fig. S6). Note that reactions start as soon as Mg^{2+} is added in the plate, before the first readings of the plate reader, thus "0" time point actually corresponds to a time point between 30 sec and 2 min.

of RNA structure dynamics and ribozyme mechanism (McDowell et al. 2010; Korman et al. 2020). However, besides radiolabeling, which has its own disadvantages, these methods are associated with direct RNA modification, which in turn can impact the structure, function, and thermodynamic stability of the measured ribozyme (Li et al. 2005; Moreira et al. 2005).

We present a novel approach to measure leaving product resulting from self-cleavage of hammerhead ribozyme by toehold-mediated strand displacement reaction (TMSDR). The proposed method separates the detection system from the ribozyme, eliminating the need for ribozyme labeling and modification. This fosters unhindered determination of cleaved-off, released fragment that can interact with the target sequence.

We conceived an oligonucleotide activated HHR, which functions as a YES logic gate. When the HHR binds to the input oligonucleotide, the HHR cleaves itself, generating an ssRNA fragment that can detach from the HHR. Detached output ssRNA interacts with the toehold present on (the 3′-end of the F-strand) of a dsDNA probe. This binding initiates a strand displacement reaction favoring the expulsion of the (Q-strand) quencher in a 5′ to 3′ direction. This process culminates in the dissociation of the quencher from the fluorophore, resulting in detectable fluorescence.

The vast majority of previous studies determine HHR cleavage using radiolabeling or product separation (Penchovsky and Breaker 2005; Perreault et al. 2011; Hammann et al. 2012; Porecha and Herschlag 2013). Product separation on denaturing gels is associated with forced detachment of an output strand from an HHR. Consequently, this approach fails to distinguish between released output and cleaved but bound output. Native gel studies can be performed to analyze cleaved and released output fragment, but, even if the presence of multiple bands associated with alternative folding of ribozymes can potentially be informative, it also makes the interpretation particularly challenging, especially in the case of allosteric ribozymes inducible by binding of oligonucleotides (Supplemental Fig. S5). Moreover, keeping the temperature constant in native gel is another hurdle to overcome. In TMSDR, the occurrence of fluorescence is a direct measure of released output. A gradual increase in cleavage activity over time was noted in both (gel and TMSDR) methods for the ribozyme. However, a decrease in rates estimated from TMSDR was observed when 2 and 14 bp were added to stem I, compared to their gel counterparts. This decrease in activity is correlated with an increase in the strength of binding between the cleaved output strand and its complement (on stem I) of the ribozyme. This decreased activity is indicative that TMSDR-based fluorescence is a measure of the concentration of the *detached* output strand, rather than the full extent of ribozymatic self-cleavage. Thus, TMSDR allows for real-time cleavage monitoring and realistic evaluation of the amount of product (RNA output) leaving the ribozyme, rather than mere cleavage. Indeed, the marked differences for standard gel assays versus TMSDR, between the HHRs with different lengths of stem I, highlight that the "k_{obs}" of TMSDR relates more to the compounded events leading to product release. This could closely reflect cleavage rate in some cases, like for the 8 bp stem I HHR, but also permits to evaluate the rate of product release in other cases, such as for the 10 bp stem I HHR (or 22 bp stem I, where there is no detectable product release). A second HHR, Mn^{2+}-HHR, was used to demonstrate the versatility of the proposed method. The second probe used Cy3 and BHQ-2 as fluorophore/quencher pair, thus demonstrating

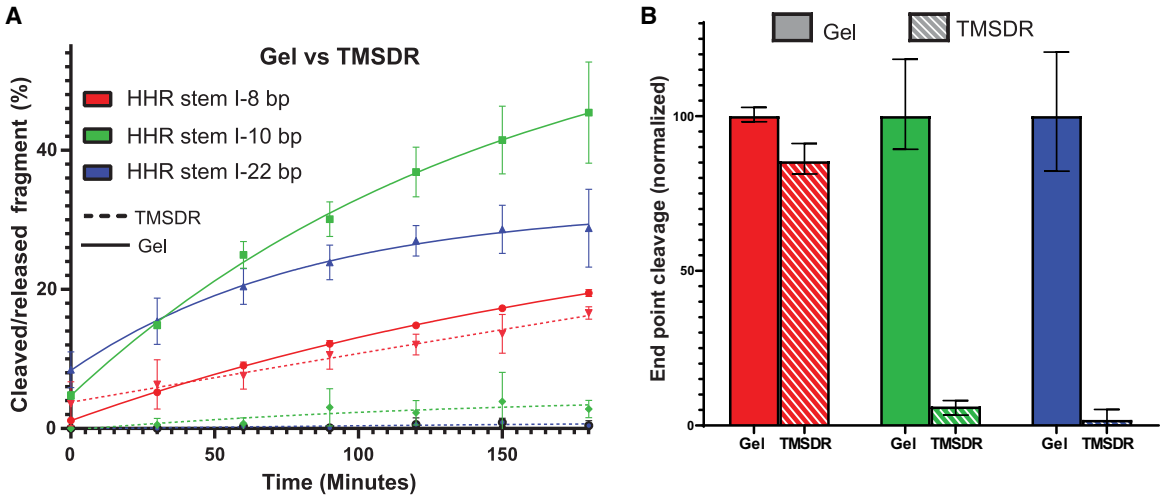

FIGURE 4. TMSDR vs. Gel cleavage analysis. (*A*) Comparison of cleavage obtained from [α-^{32}P] UTP labeled ribozymes (dotted lines) and TMSDR (solid lines). (*B*) The end point cleavage, representing total emitted fluorescence (normalized), was calculated from the graph for the original HHR (I-8) and HHR with a stem I of 10 bp (I-10) as well as 22 bp (I-22).

that different fluorophores and quenchers can be used to design probe for different ribozymes. More importantly, it illustrates the fact that faster ribozymes can also be monitored, even if rates greater than 0.2 min^{-1} cannot be precisely determined, at least with our current setup.

Our approach allows for measurement of released output strands, which may be more important than backbone scission for many synthetic biology applications. Furthermore, when complementing traditional radiolabeling methods, a TMSDR-based technique can help provide a more complete picture of cleavage activity and rate of dissociation of the cleaved products. This information can be crucial to determining and characterizing the limiting step for the development of ribozyme-based RNA circuits. TMSDR lends itself to automation more readily than radiolabeling- a trait particularly useful for eventual design of more complex RNA logic gates and circuits.

MATERIALS AND METHODS

Ribozyme sequence selection and generation

The algorithm used in this work is an extension of the one in Penchovsky and Breaker (2005). The main difference is that rather than using random search, the employed algorithm implements an *evolutionary algorithm* (EA) to search for hammerhead ribozymes that function as Yes logic gates (Kamel et al. 2020) (more details on the algorithm are in the Supplemental Material).

A second ribozyme example, which cleaves in the presence of Mn^{2+} (but not Mg^{2+}), was selected from the literature (Naghdi et al. 2020). The fact that this ribozyme is inactive in the presence of Mg^{2+} allowed us to prepare self-cleaving ribozymes easily for assays in TMSDR.

PCR assembly of DNA template

Predesigned overlapping oligodeoxynucleotides (Supplemental Fig. S1 and

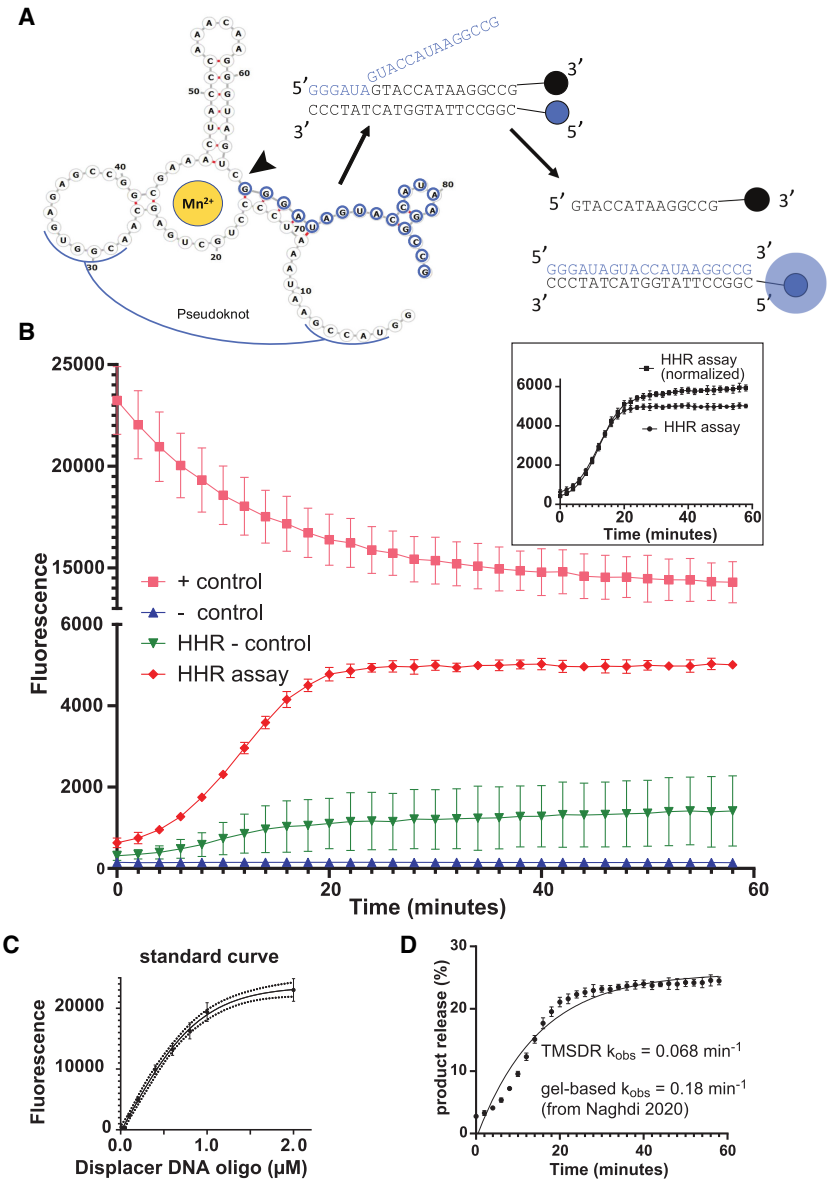

FIGURE 5. TMSDR of a ribozyme inducible by Mn^{2+}. (*A*) Mn^{2+}-HHR schematic in the presence of manganese ion. Upon cleavage, the small, released fragments (blue strand) interact with the toehold (red segment of the probe) and initiate strand displacement reaction culminating in displacement of quencher strand (orange strand), which results in fluorescence. (*B*) Manganese ribozyme TMSDR assay in the presence of 0.5 μM probe comprised of cy-3 and BHQ-2, fluorophore and quencher, respectively. (*Insets*) normalized fluorescence values for ribozyme assay. Controls are: (+) preannealed probe unquenched with excess (10 μM) displacer RNA; (–) quenched probe without displacer; (HHR –) HHR without Mn^{2+}. (*C*) Mn^{2+}-HHR probe standard curve and normalized values. Different DNA displacer concentrations from 0.01 to 2 μM were used with 0.5 μM of probe. Cy3 and BHQ-2 were used as fluorophore and quencher, respectively. (*D*) As in Figure 5C, interpolated fluorescence values were mapped using the standard curve to concentrations of released output strand. It should be noted that the ribozyme adapted from Naghdi et al. (2020) was described as having a pseudoknot (as was the original version of this HHR described previously [Perreault et al. 2011] which had an A at position 6 from the core, instead of a C in this "Mn^{2+}-HHR"). However, secondary structure prediction also suggests an alternative structure (Supplemental Fig. S7) which may impact product release. Note that reactions start as soon as Mg^{2+} is added in the plate, before the first readings of the plate reader, thus "0" time point actually corresponds to a time point between 30 sec and 2 min.

Supplemental Table S1 were assembled by PCR (BioRAD T100) using Primers F1, R1, F2, and R2 (Supplemental Fig. S1; Supplemental Table S2)). The PCR reaction was carried out in a fixed volume of 100 µL, containing primers F1 (2 µM), R1 (0.2 µM), F2 (0.2 µM), R2 (2 µM), Taq polymerase (hotStar Taq Plus from QIAGEN) with its reaction buffer at 1×, Q-solution (1× from QIAGEN), 0.2 mM of dNTPs (DGel electrosystem) and Milli-Q water. The reaction mixture was subjected to 15 min denaturation at 95°C and 15 cycles consisting of: 30 sec denaturation at 95°C, 30 sec annealing at 50°C and 30 sec extension at 72°C. PCR was validated by visualizing 5 µL of reaction mixture on 2% agarose gel containing gel red (Trans). The remaining PCR product was ethanol precipitated.

In vitro transcription and RNA purification

In vitro RNA synthesis was performed as previously described (Perreault et al. 2011), with slight modifications. When larger quantities were required, the reaction was carried out in a fixed volume of 1 mL. The reaction mixture contained 80 mM HEPES (pH 7.5), 24 mM $MgCl_2$, 40 mM dithiothreitol, 2 mM spermidine, 6 µg/mL T7 polymerase, 150 µL of PCR product (For 1 mL transcription, 10 PCR reactions (100 µL each) were pooled together, precipitated and resuspended in 150 µL Milli-Q water), 2 mM rNTPs, 1× pyrophosphatase (Roche diagnostics) and 200 U (40 U/µL) RiboLock (Thermo Fisher Scientific). The reaction mixture was incubated at 37°C for 150 min, treated with 10 U of DNase (New England Biolabs), incubated at 37°C for 30 min. The RNA was extracted with phenol-chloroform, and the aqueous phase was ethanol precipitated. The RNA was purified in 10% denaturing (8 M urea) polyacrylamide gel. The gel was revealed by UV-shadowing. The band of interest (Highest band on gel, as there was some level of cleavage during transcription) was excised and eluted in 0.3 M NaCl overnight at 4°C. The eluent was ethanol precipitated and resuspended in nuclease free water.

Radiolabeling of ribozyme using [α-^{32}P] UTP during transcription

Radiolabeling of RNA was conducted as previously described with minor modifications. Here, the reaction mixture consisted of 1× transcription buffer (see above), 15 µL of PCR product (100 µL PCR reaction ethanol precipitated and resuspended in 20 µL Milli-Q water), 2 mM of GTP, CTP, ATP, 0.125 mM UTP, 1× pyrophosphatase (Roche diagnostics) and 40 U RiboLock (Thermo Fisher Scientific) and 1 µL of [α-^{32}P] UTP (PerkinElmer) per 50 µL reaction. The reaction mixture was ethanol precipitated and analyzed in 10% denaturing polyacrylamide gel; the product was revealed by phosphorimaging (Typhoon 9500 FLA; GE Healthcare Life Sciences). The band of interest was resected and eluted in 0.3 M NaCl overnight at 4°C. The eluent was ethanol precipitated and resuspended in nuclease free water.

Preparation of fluorescent probe

Predesigned oligodeoxynucleotides were conjugated at the 5′-end with Cy5 and at the 3′-ends with Black hole quencher (Alpha DNA). The strand with the Cy5 at the 5′-end was named the "F-strand" (5′-ACAGGGTCGGACCTGGAAATCC-3′), while the strand with the Black hole quencher-3 (BHQ-3) at 3′-end was called the "Q-strand" (5′- CAGGTCCGACCCTGT-3′) (Fig. 2D). The probe was prepared in a cleavage buffer (100 mM NaCl, 50m M tris-HCl pH 7.5, 25 mM KCl) with 0.5 µM F-strand and 0.6 µM Q-strand per 10 µL reaction. The reaction was incubated in thermocycler (BioRad T100) for 3 min denaturation at 95° C, 15 min annealing at 50°C and 15 min annealing at 37°C. The same protocol was followed for Mn^{2+}-HHR probe except that the Q-strand (5′-GTACCATAAGGCCG-3′) for Mn^{2+}-HHR was labeled with BHQ-2 while F-strand (5′-CGGCCTTATGGTACTATCCC-3′) was labeled with Cy3. Both probe and quencher for Mn^{2+}-HHR were purchased from Integrated DNA technologies (IDT).

Calibration of probe and standard curve generation

The prepared probe was calibrated using ssRNA oligonucleotide (IDT) mimicking the ribozyme output (5′-GGAUUUCCAG GUCCGACCCUGU-3′). We called this strand the "R-strand" (Displacer RNA-strand). Different concentrations of R-strand, ranging from 0.05 to 2 µM were mixed with 0.5 µM preannealed probe. The reaction mixture was incubated at 37° C and analyzed using a fluorescent plate reader (Tecan M1000 Pro) at 647 nm excitation and 665 nm emission wavelengths. The probe was also calibrated using DNA displacer strand called "D-strand." Comparison of R-strand and D-strand standard curve is illustrated in Supplemental Figure S3. The TMSDR standard curve was also generated at three time points to estimate whether TMSDR was the limiting step in the measurements (Supplemental Fig. S4). The same protocol was followed to calibrate the Mn^{2+}-HHR probe with its corresponding D-strand (5′-GGGATAGTACCATAA GGCCG-3′). For Mn^{2+} probe, 550 nm excitation and 564 nm emission wavelengths were used.

Analysis of hammerhead ribozyme kinetics on polyacrylamide gel

Ribozyme kinetics were assayed using a labeled [α-^{32}P] UTP ribozyme. The reaction was performed in a fixed volume of 10 µL, containing 100 mM NaCl, 50 mM Tris-HCl pH-7.5, 25 mM KCl, 10 mM $MgCl_2$, 10 µM input oligodeoxynucleotide, and 1 µL of the labeled ribozyme. The reaction was started by adding $MgCl_2$. The reaction was incubated at 37°C. Sequentially, the aliquots of reactions were stopped at 30 min intervals using denaturation buffer (80% formamide, 0.5 mM EDTA, 0.02% bromophenol blue, and 0.02% xylene cyanol). The samples were analyzed on 10% denaturing polyacrylamide gel, the gel was developed by phosphorimaging and the band intensity was determined using ImageQuant software (GE Healthcare Life Sciences). Both bands resulting from cleavage were quantified and their sum was divided by the total of the three bands corresponding to cleaved fragments and full length.

Analysis of hammerhead ribozyme kinetics with strand displacement

A preannealed probe was used to evaluate HHR cleavage kinetics. Here, 0.5 µM of a preannealed probe was mixed with 10 mM

$MgCl_2$, 10 µM input oligodeoxynucleotide, and 1 µM ribozyme per 10 µL reaction, for Mn^{2+}-HHR reactions 0.3 mM $MnCl_2$ was used to initiate the reaction. The reaction mixture was incubated at 37°C. The fluorescence emitted was measured using a fluorescent plate reader (Tecan M1000 Pro). Readings were taken every 30 min.

GraphPad Prism was used using first order decay rate constant determination to calculate k_{obs} for both the TMSDR and gel-based assays. In the case of TMSDR-based assays, because the plateau was estimated to be ~236% (even if theoretical maximum is 100%) for the 8 bp stem HHR, plateaus were fixed at 100%.

SUPPLEMENTAL MATERIAL

Supplemental material is available for this article.

ACKNOWLEDGMENTS

The authors wish to thank Ms. Sabrine Najeh for technical assistance and helpful discussion. J.B.K. and N.K. received fellowships from Natural Sciences and Engineering Council of Canada (NSERC) SynBioApps program (CREATE-511601-2018). J.P. is a junior 2 FRQS research scholar. Other funding, including for publication charge: NSERC (RGPIN-2019-06403).

Received May 2, 2021; accepted October 27, 2021.

REFERENCES

Auslander S, Fuchs D, Hurlemann S, Auslander D, Fussenegger M. 2016. Engineering a ribozyme cleavage-induced split fluorescent aptamer complementation assay. *Nucleic Acids Res* **44:** e94. doi:10.1093/nar/gkw117

Celander DW, Cech TR. 1991. Visualizing the higher order folding of a catalytic RNA molecule. *Science* **251:** 401. doi:10.1126/science.1989074

Chi Y-I, Martick M, Lares M, Kim R, Scott WG, Kim S-H. 2008. Capturing hammerhead ribozyme structures in action by modulating general base catalysis. *PLOS Biol* **6:** e234. doi:10.1371/journal.pbio.0060234

Debiais M, Lelievre A, Smietana M, Müller S. 2020. Splitting aptamers and nucleic acid enzymes for the development of advanced biosensors. *Nucleic Acids Res* **48:** 3400–3422. doi:10.1093/nar/gkaa132

Duose DY, Schweller RM, Zimak J, Rogers AR, Hittelman WN, Diehl MR. 2012. Configuring robust DNA strand displacement reactions for in situ molecular analyses. *Nucleic Acids Res* **40:** 3289–3298. doi:10.1093/nar/gkr1209

Furth J, Tullis JL. 1956. Carcinogenesis by radioactive substances. *Cancer Res* **16:** 5–21.

Hammann C, Luptak A, Perreault J, de la Pena M. 2012. The ubiquitous hammerhead ribozyme. *RNA* **18:** 871–885. doi:10.1261/rna.031401.111

Kamel N, Kharma N, Abu-baker A, Rouleau G, Bailey A. 2020. Evolutionary design and experimental evaluation of selective hammerhead ribozymes. In *IEEE 20th international conference on bioinformatics and bioengineering (BIBE)*, Cincinnati, Ohio.

Kerpedjiev P, Hammer S, Hofacker IL. 2015. Forna (force-directed RNA): simple and effective online RNA secondary structure diagrams. *Bioinformatics* **31:** 3377–3379. doi:10.1093/bioinformatics/btv372

Khodakov DA, Khodakova AS, Huang DM, Linacre A, Ellis AV. 2015. Protected DNA strand displacement for enhanced single nucleotide discrimination in double-stranded DNA. *Sci Rep* **5:** 8721. doi:10.1038/srep08721

Korman A, Sun H, Hua B, Yang H, Capilato JN, Paul R, Panja S, Ha T, Greenberg MM, Woodson SA. 2020. Light-controlled twister ribozyme with single-molecule detection resolves RNA function in time and space. *Proc Natl Acad Sci* **117:** 12080–12086. doi:10.1073/pnas.2003425117

Li N, Yu C, Huang F. 2005. Novel cyanine-AMP conjugates for efficient 5′ RNA fluorescent labeling by one-step transcription and replacement of [γ-32P]ATP in RNA structural investigation. *Nucleic Acids Res* **33:** e37. doi:10.1093/nar/gni036

McDowell SE, Jun JM, Walter NG. 2010. Long-range tertiary interactions in single hammerhead ribozymes bias motional sampling toward catalytically active conformations. *RNA* **16:** 2414–2426. doi:10.1261/rna.1829110

Mitra J, Ha T. 2019. Nanomechanics and co-transcriptional folding of Spinach and Mango. *Nat Commun* **10:** 4318. doi:10.1038/s41467-019-12299-y

Moreira BG, You Y, Behlke MA, Owczarzy R. 2005. Effects of fluorescent dyes, quenchers, and dangling ends on DNA duplex stability. *Biochem Biophys Res Commun* **327:** 473–484. doi:10.1016/j.bbrc.2004.12.035

Moreira BG, You Y, Owczarzy R. 2015. Cy3 and Cy5 dyes attached to oligonucleotide terminus stabilize DNA duplexes: predictive thermodynamic model. *Biophys Chem* **198:** 36–44. doi:10.1016/j.bpc.2015.01.001

Murray JB, Terwey DP, Maloney L, Karpeisky A, Usman N, Beigelman L, Scott WG. 1998. The structural basis of hammerhead ribozyme self-cleavage. *Cell* **92:** 665–673. doi:10.1016/S0092-8674(00)81134-4

Naghdi MR, Boutet E, Mucha C, Ouellet J, Perreault J. 2020. Single mutation in hammerhead ribozyme favors cleavage activity with manganese over magnesium. *Noncoding RNA* **6:** 14. doi:10.3390/ncrna6010014

Nelson JA, Uhlenbeck O. 2008. Hammerhead redux: does the new structure fit the old biochemical data? *RNA* **14:** 605–615. doi:10.1261/rna.912608

Penchovsky R, Breaker RR. 2005. Computational design and experimental validation of oligonucleotide-sensing allosteric ribozymes. *Nat Biotechnol* **23:** 1424–1433. doi:10.1038/nbt1155

Perreault J, Weinberg Z, Roth A, Popescu O, Chartrand P, Ferbeyre G, Breaker RR. 2011. Identification of hammerhead ribozymes in all domains of life reveals novel structural variations. *PLoS Comput Biol* **7:** e1002031. doi:10.1371/journal.pcbi.1002031

Porecha R, Herschlag D. 2013. RNA radiolabeling. *Methods Enzymol* **530:** 255–279. doi:10.1016/B978-0-12-420037-1.00014-2

Prody GA, Bakos JT, Buzayan JM, Schneider IR, Bruening G. 1986. Autolytic processing of dimeric plant virus satellite RNA. *Science* **231:** 1577. doi:10.1126/science.231.4745.1577

Qian L, Winfree E. 2011. Scaling up digital circuit computation with DNA strand displacement cascades. *Science* **332:** 1196. doi:10.1126/science.1200520

Qian L, Winfree E, Bruck J. 2011. Neural network computation with DNA strand displacement cascades. *Nature* **475:** 368–372. doi:10.1038/nature10262

Ravan H, Amandadi M, Hassanshahian M, Pourseyedi S. 2020. Dual catalytic DNA circuit-induced gold nanoparticle aggregation: an enzyme-free and colorimetric strategy for amplified detection of nucleic acids. *Int J Biol Macromol* **154:** 896–903. doi:10.1016/j.ijbiomac.2020.03.059

Sclavi B, Sullivan M, Chance MR, Brenowitz M, Woodson SA. 1998. RNA folding at millisecond intervals by synchrotron hydroxyl radical footprinting. *Science* **279:** 1940–1943. doi:10.1126/science.279.5358.1940

Scott WG, Horan LH, Martick M. 2013. The hammerhead ribozyme: structure, catalysis, and gene regulation. *Prog Mol Biol Transl Sci* **120:** 1–23. doi:10.1016/B978-0-12-381286-5.00001-9

Simmel FC, Yurke B, Singh HR. 2019. Principles and applications of nucleic acid strand displacement reactions. *Chem Rev* **119:** 6326–6369. doi:10.1021/acs.chemrev.8b00580

Singh KK, Parwaresch R, Krupp G. 1999. Rapid kinetic characterization of hammerhead ribozymes by real-time monitoring of fluorescence resonance energy transfer (FRET). *RNA* **5:** 1348–1356. doi:10.1017/S1355838299991185

Šulc P, Ouldridge TE, Romano F, Doye JPK, Louis AA. 2014. Modelling toehold-mediated RNA strand displacement. *Biophys J* **108:** 1238–1247.

Wang B, Thachuk C, Ellington AD, Winfree E, Soloveichik D. 2018. Effective design principles for leakless strand displacement systems. *Proc Natl Acad Sci* **115:** E12182. doi:10.1073/pnas.1806859115

Wittmann A, Suess B. 2011. Selection of tetracycline inducible self-cleaving ribozymes as synthetic devices for gene regulation in yeast. *Mol BioSyst* **7:** 2419–2427. doi:10.1039/c1mb05070b

Yurke B, Turberfield AJ, Mills AP, Simmel FC, Neumann JL. 2000. A DNA-fuelled molecular machine made of DNA. *Nature* **406:** 605–608. doi:10.1038/35020524

Zhang DY, Winfree E. 2009. Control of DNA strand displacement kinetics using toehold exchange. *J Am Chem Soc* **131:** 17303–17314. doi:10.1021/ja906987s

MEET THE FIRST AUTHOR

Jay Bhakti Kapadia

***Meet the First Author(s)* is a new editorial feature within *RNA*, in which the first author(s) of research-based papers in each issue have the opportunity to introduce themselves and their work to readers of *RNA* and the RNA research community. Jay Kapadia is the first author of this paper, "Toehold-mediated strand displacement to measure released product from self-cleaving ribozymes." Jay obtained a bachelor's degree in Biotechnology from Uka Tarsadia University, India and a master's degree in Electrical and Computer Engineering from Concordia University, Montreal. Jay is currently working/studying as a PhD student in collaboration with the INRS-Armand Frappier Institute and Galenvs Biosciences, focusing on harnessing toehold sensors to develop diagnostic kits for pathogen nucleic acid detection.**

What are the major results described in your paper and how do they impact this branch of the field?

The major findings provided in the paper are the following: (1) A methodology to measure the cleaved product from self-cleaving ribozymes without labeling. (2) The comparison gives an actual picture of ribozyme cleavage and cleaved fragment dissociation in real time without gel separation techniques. (3) Native gel results included in the Supplemental Material demonstrate the complexity of using radiolabeling to determine cleaved and released fragments from self-cleaving ribozymes. The methodology presented in the article allows researchers in the field to characterize RNA-based logic gates without using radiolabeling or gel separation. The protocol permits users to monitor multiple ribozymes in real time.

What led you to study RNA or this aspect of RNA science?

RNA enzymes, also known as ribozymes, can catalyze strand scission reaction without the help of protein molecules. These enzymes can be tailored to work as different logic gates that can detect specific signals. Examples of these signals include but are not restricted to single-stranded nucleic acid sequences, small chemical molecules or other protein molecules. I was interested in developing an RNA-based logic gate system to amplify the signal (RNA-based amplifier).

During the course of these experiments, were there any surprising results or particular difficulties that altered your thinking and subsequent focus?

In one of our toehold-mediated strand displacement reaction experiments, contrary to our expectations we noticed a lower signal with one of the tested ribozymes. Upon further analysis, we observed that the cleaved fragment had a T_m higher than 37°C. This led us to thinking about the fragment cleaving and dissociating instead of just cleaving. This stands in stark contrast to denaturing gel separation methodology, as it only takes into account cleavage and not cleaved and released fragments.

What are some of the landmark moments that provoked your interest in science or your development as a scientist?

Science has always been a part of my life. From childhood, I was very curious about the mechanisms of natural phenomena, especially of living beings. This led me to choose biology as my major in high school. Later, I attended seminars, company site visits, and field trips while at Uka Tarsadia University (India). While at the university, lectures in basic molecular biology piqued my interest toward this field. My bachelor's in biotechnology can be marked as a milestone for my career development as a scientist.

Continued

If you were able to give one piece of advice to your younger self, what would that be?

I would say make plans but don't worry if you have to make changes to them. Be dynamic and have a mindset to adapt to difficult situations and make the most out of it. Lastly, have fun, do not overwork yourself as having fun is as important as following your passion.

Are there specific individuals or groups who have influenced your philosophy or approach to science?

My parents, my supervisors (especially Dr. Jonathan Perreault, Dr. Christian Tebid Tebid, and Dr. Jamal Daoud). Their perceptions about life, problem solving, troubleshooting, managing people, critical thinking and views on science have greatly fine-tuned my overall way of rationalization.

What are your subsequent near- or long-term career plans?

Prospectively, I envisage a career involving a postdoctoral fellowship in the United States.